Ab Initio and DFT Study of All Mono-, Di-, Tri-, and Tetrafluoropyrroles and Their Cations: Predicting Structural, Spectroscopic, Electropolymerization, and Electrochemical Properties

Hassan Sabzyan*,† and Abdollah Omrani‡

Department of Chemistry, University of Isfahan, Isfahan 81746-73441, I. R. Iran, and Department of Chemistry, University of Mazandaran, Babolsar, P.O. Box 453, I. R. Iran

Received: January 21, 2003; In Final Form: June 11, 2003

Electronic, structural, and spectroscopic properties of the ground-state neutral and singly ionized mono-, di-, tri-, and tetrafluoropyrroles are studied using ab initio and density functional theory quantum mechanical methods. The effects of the number and position of the substituents on the electrochemical properties of the pyrrole ring have been studied. Using the optimized structures obtained for these molecules and their cations, IR and NMR spectra have been calculated and analyzed. The results of this study, including charge- and spin-density distribution analyses, show that among all of these compounds 3-fluoropyrrole and 3,4-difluoropyrrole have the most suitable conditions for electropolymerization.

1. Introduction

In recent years, intrinsic conducting polymers with conjugated double bonds have attracted much attention as advanced materials. Among these conducting polymers, polypyrroles (PPY) and related derivatives are especially promising for commercial applications because of their good environmental stability and higher conductivity. PPYs have been used as biosensors,[1,2] gas sensors,[3,4] microactuators,[5] data storage,[6] polymer batteries, electronic devices, and functional membranes.[7−11] Furthermore, the electrochemical process parameters affecting the properties of PPY coatings have also been investigated.[12] PPY-based polymer blends can prevent the corrosion of metals.[13] Also, structural studies on PPYs through an ab initio evaluation of binding[14] and a Monte Carlo growth approach to branch formation have been reported.[15] The energy differences among different types of structures suggest that a great deal of branching is probable. The approximate probability function generated in this manner has been used in a statistical mechanical approach to estimate the extent of bonding involving β carbons (position C5 in Figure 1) as well as branching in PPYs.[14] The statistical analysis of the growth process has also shown that branching occurs even for very short chains. The extent of branching does not depend on the chain length. However, it is a slowly varying function of temperature.[15] The anisotropic character of the interaction energy of the pyrrole dimer has also been studied previously using ab initio theoretical calculations.[16] Several investigations have been performed to observe the effects of various parameters such as solvent, electrolyte, and monomer choices and polymerization temperature on the stability and conductivity of the synthesized PPYs.[17−18]

Density-functional theory (DFT) is a ground-state theory that is valid for neutral and charged species as well as for the lowest state of each electronic symmetry.[19−21] DFT methods have been used as a powerful tool of computational study on a variety of molecules, especially those that could not be studied by either HF-SCF methods because of the poor evaluation of the predicted molecular properties or MPn perturbation theory methods because of the prolonged time of calculations.[22−23]

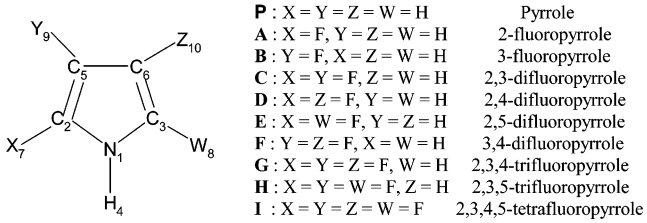

P : X = Y = Z = W = H	Pyrrole
A : X = F, Y = Z = W = H	2-fluoropyrrole
B : Y = F, X = Z = W = H	3-fluoropyrrole
C : X = Y = F, Z = W = H	2,3-difluoropyrrole
D : X = Z = F, Y = W = H	2,4-difluoropyrrole
E : X = W = F, Y = Z = H	2,5-difluoropyrrole
F : Y = Z = F, X = W = H	3,4-difluoropyrrole
G : X = Y = Z = F, W = H	2,3,4-trifluoropyrrole
H : X = Y = W = F, Z = H	2,3,5-trifluoropyrrole
I : X = Y = Z = W = F	2,3,4,5-tetrafluoropyrrole

Figure 1. All possible mono-, di-, tri-, and tetrafluoropyrrole isomers studied in this research.

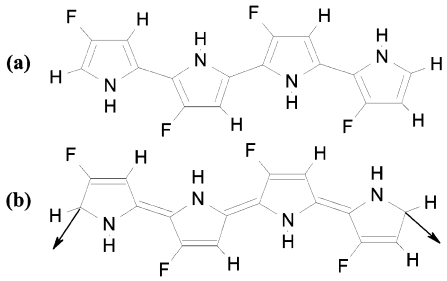

Figure 2. (a) Molecular structure of tetra(3-fuoropyrrole), the **B** tetramer, studied in this research and (b) quinoid structure of the propagating cation radical polymer chain.

The aims of the present research are (1) to study the electronic and structural properties of all fluoropyrrole monomers (shown in Figure 1) and their singly ionized cations using ab initio and DFT-B3LYP methods and (2) to compare the calculated properties of these monomers and their cations with those of the tetramer of 3-fluoropyrrole, shown in Figure 2, and its cation. The electropolymerization of monomers and characteristics of the products (conductivity and solubility) are related to the stability of their cation radicals, which itself is closely dependent on the type and configuration of the substituents on the pyrrole ring. Vibrational frequencies and NMR shielding constants

* Corresponding author. E-mail: sabzyan@sci.ui.ac.ir.
† University of Isfahan.
‡ University of Mazandaran.

10.1021/jp034155f CCC: $25.00
Published on Web 07/26/2003

TABLE 1: Ground-State Electronic Energies of Formation (eq 1) Calculated for Representative Mono-, Di-, Tri-, and Tetrafluoropyrroles Using RHF, MP2, and DFT-B3LYP Levels of Theory with the 6-31G Basis Set**

molecule (Figure 1)	ΔE_{elec} (kcal/mol)		
	RHF	MP2	B3LYP
A	138.3	−30.3	−37.4
C	99.4	−66.3	−73.8
G	59.9	N. A.	−110.9
I	21.5	N. A.	−146.1

analyses carried out on the optimized structures can also be used to characterize and predict molecular and spectroscopic properties.

2. Computational Procedures

As in complex systems, identifying the minimum-energy configurations is quite difficult because of the presence of several local minima on the energy surface. Initially, structures of representative mono-, di-, tri-, and tetra-fluoropyrroles were fully optimized using gradient procedures at restricted Hartree−Fock RHF, Møller−Plesset perturbation theory MP2, and hybrid density functional B3LYP levels of theory using the 6-31G** basis set as implemented in the Gaussian 94 program package (G94W).[24] The geometries are optimized using standard gradient techniques with default parameters set in G94W. The natures of the optimized stationary points were all characterized by frequency calculations at the same level of theory with the same basis set. The analysis of the results showed that all methods characterized all of the optimized structures obtained in this study as minima on the potential energy surface without any negative mode. The zero-point energy corrections are performed using a scaling factor of 0.89.[25] A preliminary basis set test carried out at the RHF level of theory showed that 6-31G** is the best basis set that can be used within our available hardware/software facilities in a reasonable time.

Effects of the level of theory (and the effect of the basis set in the preliminary study) on the calculated electronic energies corresponding to the optimized structures are studied on the basis of the changes in the ground-state electronic energy in formation reaction **1**.

$$4C(\text{graph}) + ((5-n)/2)H_2(g) + (1/2)N_2(g) + (n/2)F_2(g) \rightarrow C_4H_{5-n}NF_n(g) \quad (1)$$

All of the required electronic energies have been calculated for the stable forms of the constituting elements using the same level of theory and basis set used for the calculations on the related molecule. The vaporization energy of graphite has been obtained from the experimental results reported in the literature.[26] The calculated values of the electronic energies of formation are given in Table 1.

Because MP2 calculations could not be carried out for some of these representative fluoropyrroles because of software and hardware limitations, a comparative study was not applicable on the basis of MP2 calculations. Furthermore, DFT-B3LYP calculations are more powerful in the prediction of electronic properties and optimized geometries of this series of compounds with π-electron systems than simple RHF/UHF calculations are. Hence, we have selected DFT-B3LYP as the method of choice for the present study. All of the possible fluoropyrroles studied in this work are presented in Figure 1.

3. Results and Discussion

3.1. Structural Analysis of Fluoropyrroles. In this section, the electronic and structural properties of ground-state fluoropyrroles and their related cation radicals have been studied. Because of the stabilizing effects of the delocalization of nitrogen nonbonding p electrons participating in the π-conjugation system of the pyrrole ring, it is expected that the favored structure corresponds to a perpendicular orientation of the nitrogen 2p nonbonding orbital with respect to the pyrrole ring molecular plane. In agreement with this expectation, the results of the present calculations show that all fluoropyrroles have planar structures (i.e., the optimized values of all dihedral angles for all of the species studied in this research are either 0 or 180°). The optimized structural parameters obtained at the B3LYP/6-31G** level of theory for different fluoropyrroles are listed in Table 2.

To predict the bonding-characteristic behavior of the fluoropyrrole rings in their corresponding polymer chains and to determine the extent of the π-conjugation character of these polymers, we have used the F_n coefficient defined in eq 2 for each pyrrole ring in the isolated fluoropyrroles and in the tetramer of 3-fluoropyrrole.

$$F_n = \frac{2R56}{R25 + R36} \quad (2)$$

In this equation, R56 is the length of the C5−C6 bond (formally a single bond) in the *n*th pyrrole ring, and [(R25 + R36)/2] is the average length of the C2−C5 and C3−C6 bonds (formally double bonds) in the same pyrrole ring.[27] The value of the F_n coefficient gives a measure of the relative importance of the aromatic character with respect to the quinoid character of each derivative. The quinoid term refers to a structure in which the C5−C6 and inter-ring bond has greater double-bond character than in the standard aromatic configuration. The calculated values of the F_n coefficient for all fluoropyrroles and their cations are listed in Table 2. As shown in this table, molecules **B** and **F** and their cations have the smallest values of the F_n coefficient. Therefore, the quinoid character of monomers **B** and **F** is greater than that of other fluoropyrroles. It can then be concluded that for the cation polymer structure of these two monomers the quinoid structure is more probable. This shows that double bonds in these molecules are more delocalized. Consequently, quinoid structures, as in Figure 2b, involved in polymer chain growth are more probable for these monomers. This means that, compared with other fluoropyrroles, these two monomers have a higher capacity for electropolymerization as well as higher electric conductance.

3.2. Structural Analysis of Tetra(3-fluoropyrrole), the B Tetramer. Results of the calculations reported in a previous work show that an infinite neutral chain of a pyrrole ring in a 3-D periodic arrangement is planar.[15] This can be explained in terms of attractive interactions between properly oriented electric dipole moments of adjacent rings. Therefore, it can be assumed that the **B** tetramer and its cation are planar. On the basis of this fact, we have optimized structures of both the neutral and singly ionized **B** tetramer upon setting a planar initial structure (i.e., planar (α-α′) s-trans conformation with an alternate orientation of the pyrrole rings). The optimized structure of the **B** tetramer is shown in Figure 2a.

An analysis of the values of the F_n coefficient of the **B** tetramer and its cation, reported in Table 3, shows that for both the neutral tetramer and its cation the center of the chain has greater quinoid character than the terminal rings have. The radical cation of the **B** tetramer shows a quinoid structure localized in the central part of the chain, whereas the aromatic conjugation in this oligomer is concentrated mainly on the terminal rings. Thus, the only possible rotations are those around

TABLE 2: B3LYP/6-31G Optimized Values of (a) Bond Lengths and the F_n Coefficient and (b) Bond Angles for Fluoropyrroles[a]**

(a) Bond Lengths (Å) and F_n Coefficients

molecule	N1−C2	N1−C3	C2−C5	C3−C6	C5−C6	F_n
pyrrole	1.375	1.375	1.378	1.378	1.425	1.034
	1.363	*1.363*	*1.433*	*1.433*	*1.374*	*0.958*
A	1.365	1.385	1.368	1.374	1.431	1.043
	1.363	*1.365*	*1.425*	*1.431*	*1.376*	*0.963*
B	1.379	1.371	1.375	1.380	1.416	1.028
	1.337	*1.395*	*1.455*	*1.395*	*1.385*	*0.972*
C	1.369	1.380	1.371	1.377	1.420	1.033
	1.344	*1.387*	*1.449*	*1.405*	*1.380*	*0.967*
D	1.360	1.392	1.372	1.371	1.424	1.038
	1.379	*1.352*	*1.402*	*1.447*	*1.380*	*0.969*
E	1.376	1.376	1.364	1.364	1.440	1.056
	1.366	*1.366*	*1.421*	*1.421*	*1.380*	*0.971*
F	1.376	1.376	1.376	1.376	1.416	1.029
	1.365	*1.364*	*1.43*	*1.431*	*1.379*	*0.964*
G	1.365	1.387	1.372	1.372	1.422	1.029
	1.359	*1.372*	*1.433*	*1.426*	*1.380*	*0.965*
H	1.382	1.370	1.366	1.367	1.431	1.029
	1.356	*1.379*	*1.441*	*1.404*	*1.382*	*0.971*
I	1.377	1.377	1.368	1.368	1.431	1.029
	1.367	*1.367*	*1.427*	*1.427*	*1.384*	*0.969*

(b) Bond Angles (deg)

molecule	C2−N1−C3	C2−N1−H4	C3−N1−H4	N1−C2−C5	N1−C2−X	N1−C3−W
pyrrole	109.7	125.1	125.1	107.6	121.1	121.1
	109.0	*125.4*	*125.4*	*108.3*	*121.7*	*121.7*
A	108.3	124.6	126.9	110.2	119.0	120.9
	107.5	*125.3*	*127.0*	*110.3*	*120.6*	*121.5*
B	110.2	124.6	125.1	105.9	122.8	121.2
	109.6	*125.3*	*124.9*	*106.0*	*124.4*	*120.6*
C	108.9	124.2	126.7	108.2	120.4	121.0
	107.9	*125.4*	*126.5*	*108.2*	*123.3*	*120.5*
D	108.9	124.7	126.3	110.6	119.1	122.5
	108.1	*125.0*	*126.8*	*111.5*	*119.4*	*123.8*
E	106.9	126.5	126.5	110.1	118.6	118.6
	106.1	*126.9*	*126.9*	*110.4*	*120.4*	*120.4*
F	110.7	124.6	124.6	106.6	122.7	122.7
	109.4	*125.3*	*125.3*	*108.*	*123.2*	*123.2*
G	109.5	124.2	126.1	108.9	120.5	122.4
	108.0	*125.3*	*126.5*	*109.8*	*122.1*	*122.7*
H	107.6	125.9	126.4	108.1	119.9	118.8
	106.7	*126.7*	*126.5*	*108.4*	*122.6*	*119.4*
I	108.4	125.7	125.7	108.7	120.0	120.0
	107.0	*126.4*	*126.4*	*109.8*	*121.6*	*121.6*

[a] Corresponding values for the related cations are given in the lower row with italic fonts. See Figure 1 for definitions of bond lengths and angles.

TABLE 3: Values of the F_n Coefficient[a] and Interring Bond Length $R_{n,n+1}$ for the B3LYP/6-31G Optimized Structure of Tetra(3-Fluoropyrrole) (B Tetramer) and Its Cation with a Planar Conformation[b]**

	neutral **B** tetramer		**B**-tetramer cation			
n	F_n	$R_{n,n+1}$ (Å)	F_n	$R_{n,n+1}$ (Å)	charge	spin density
1	1.020	1.440	0.996	1.415	0.297	0.247
2	1.011	1.438	0.973	1.407	0.264	0.325
3	1.011	1.440	0.977	1.420	0.236	0.275
4	1.018		1.005		0.180	0.152

[a] *n* is the progressive number of the ring in the tetramer. [b] In the last two columns, the overall electric charge and spin density of each ring of the **B**-tetramer cation have been listed, respectively.

the terminal inter-ring C−C bonds that maintain their single-bond character. This result is confirmed by inspecting the values of the F_n coefficient and the inter-ring bond lengths reported in Table 3. It is obvious that the ionization of the **B** tetramer induces structural modifications. A typical quinoid structure of a propagating cation radical polymer chain is shown in Figure 2b.

3.3. Charge- and Spin-Distribution Analysis. Using Mulliken population analysis, the net atomic electric charges in this series of fluoropyrroles and their cations have been calculated and reported in Table 4. In addition, the spin-density distribution over the ring atoms of the fluoropyrrole cation radicals have been calculated and presented in Table 5. The calculated net electric charges and spin densities of all four rings of the **B** tetramer and its cation radical have been listed in Table 3. From the analysis of these data, one can draw the following conclusions.

(A) For all fluoropyrroles and their cations, the positive charge is distributed mainly on the α-carbon (C2 position in Figure 1), whereas spin density is distributed mainly on the α′-carbon (C3 position in Figure 1). This behavior can be expected because the distributed charge is positive and the spin density is carried by the negative charge of the electrons.

(B) In both series of molecules and their cation radicals, charge- and spin-density distributions have similar trends with the number and position of the substituted fluorine atoms. However, charge distribution has lower symmetry for cation radical series.

TABLE 4: Charge Distribution on Nitrogen and Carbon Atoms in the B3LYP/6-31G Optimized Structures of Pyrrole and Fluoropyrroles (and Their Cations)**

molecule	$-\delta_N$	δ_{C2}	δ_{C3}	δ_{C5}	δ_{C6}
pyrrole	0.048 (*0.456*)	0.070 (*0.198*)	0.070 (*0.198*)	−0.128 (*−0.075*)	−0.128 (*−0.075*)
A	0.517 (*0.490*)	0.462 (*0.598*)	0.067 (*0.192*)	−0.156 (*0.086*)	−0.132 (*−0.083*)
B	0.493 (*0.462*)	0.029 (*0.184*)	0.081 (*0.173*)	0.267 (*0.351*)	−0.165 (*−0.110*)
C	0.523 (*0.491*)	0.424 (*0.586*)	0.074 (*0.174*)	0.247 (*0.341*)	−0.164 (*−0.114*)
B	0.527 (*0.499*)	0.483 (*0.597*)	0.025 (*0.178*)	−0.199 (*−0.130*)	0.274 (0.348)
E	0.549 (*0.525*)	0.464 (*0.597*)	0.464 (*0.598*)	−0.160 (*−0.094*)	−0.160 (*−0.094*)
F	0.501 (*0.474*)	0.038 (*0.177*)	0.038 (*0.177*)	0.238 (*0.317*)	0.238 (*0.317*)
G	0.533 (*0.508*)	0.442 (*0.590*)	0.029 (*0.162*)	0.213 (*0.306*)	0.250 (*0.324*)
H	0.557 (*0.534*)	0.423 (*0.581*)	0.480 (*0.597*)	0.254 (*0.343*)	−0.198 (*−0.135*)
I	0.565 (*0.543*)	0.436 (*0.581*)	0.436 (*0.582*)	0.225 (*0.312*)	0.225 (*0.127*)

TABLE 5: Distribution of Spin Density over Nitrogen and Carbon Atoms in the B3LYP/6-31G Optimized Structures of Pyrrole and Fluoropyrrole Cations**

cation	N	C2	C3	C5	C6
pyrrole	−0.118	0.537	0.577	0.046	0.046
A	−0.098	0.385	0.542	0.096	0.034
B	−0.059	0.505	0.442	0.222	−0.134
C	−0.087	0.400	0.490	0.206	−0.111
D	−0.058	0.338	0.562	−0.049	0.127
E	−0.088	0.392	0.392	0.089	0.089
F	−0.108	0.552	0.552	0.003	0.006
G	−0.094	0.399	0.565	0.067	−0.026
H	−0.075	0.428	0.360	0.151	−0.034
I	−0.086	0.417	0.417	0.037	0.037

(C) For the singly ionized **B** tetramer, the positive charge is localized mainly on the two end rings whereas the spin density is distributed primarily on the central rings of the chain.

On the basis of the results obtained in this study, one can conclude that among all of these fluoropyrroles, 3-fluoropyrrol **B** and 3,4-difluoropyrrole **F** can be electropolymerized much easier under suitable conditions. The higher positive charge on the C3 carbon atom for monomer **B** shows that, possibly, the electropolymerization rate for monomer **B** is greater than that for monomer **F**. Furthermore, the higher negative charge on the β'-carbon (C6 position in Figure 1) in monomer **B** suggests that cationic polymerization of monomer **B** from the β'-carbon is not possible. In other words, propagation of the polymer chain through the α'-carbon is the favored choice. Therefore, it can be predicted that compared with the polymers of other fluoropyrroles, the **B** polymer has less-twisted junctions. Consequently, it can be said that compared with other fluoropyrroles the electric conductivity of polymer blends obtained from the **B** monomer is higher.

3.4. Electric Dipole Moments. Orientations of the polymer chains in the condensed phase are the most important parameters affecting the electric charge transport properties of polymers so that the electrical conductivity of a polymer chain is altered when its orientation and consequently its symmetry and nonisotropic interactions are changed. These overall interactions can well be expressed in terms of the interactions between local dipole moments of monomers. The local alignment of monomers' dipole moments in solution with respect to the orientation of the polymer chain determines the electrochemical properties of the polymer formed on the electrode surface. In addition, the orientation of monomer in the double layer of the solution in the electropolymerization cell depends on both the size and direction of the dipole moment vectors of both the monomers and the polymer chain. It is therefore necessary to study the dipole moments of these fluoropyrroles to be able to predict their electropolymerization properties. The size of the dipole moment vector and its components calculated for fluoropyrroles in this study are presented in Table 6. The analysis carried out on the calculated dipole moments shows that the size and direction of the dipole moment vector depend mainly on the position (symmetry) of substituents rather than on the number of substituents. Furthermore, the orientation of the dipole moment vector is toward the nitrogen atom for all fluoropyrroles. It can also be seen from Table 6 that the size of the dipole moment vector for monomer **F** is greater than that for other monomers studied in this research. In addition, monomer **B** has a greater dipole moment than pyrrole has. It can then be concluded that the solubility of 3-fluoropyrrole **B** and 3,4-difluoropyrrole **F** in polar solvents is higher than that of pyrrole. Thus, these two monomers are better candidates for electropolymerization.

TABLE 6: Electric Dipole Moments, Polarizability Tensor Elements, and Ionization Potentials Calculated at the B3LYP/6-31G Level of Theory for the Optimized Structures of Pyrrole and Fluoropyrroles[a]**

	electric dipole moment (D)			polarizabilities (Å)				ionization potential (eV)
molecule	μ_x	μ_y	μ_{tot}	α_{xx}	α_{yy}	α_{zz}	α_{xy}	IP
pyrrole	0	1.90	1.90	53.10	52.30	18.24	0.00	7.81
A	−1.63	−0.76	1.79	52.30	52.72	19.12	0.16	7.77
B	−0.98	−2.90	3.07	52.95	52.56	19.16	−0.29	7.92
C	−3.14	0.32	3.16	52.84	52.91	20.15	0.40	7.86
D	−1.27	−2.08	2.44	52.81	52.59	20.02	−0.16	7.91
E	0	0.94	0.94	52.54	52.39	20.00	0.00	7.75
F	0	3.93	3.93	52.96	53.02	20.16	0.04	8.20
G	−1.16	−3.42	3.61	53.36	53.07	21.12	−0.04	8.11
H	−2.16	−0.09	2.16	52.88	52.97	21.01	0.15	7.85
I	0	2.97	2.97	53.51	53.51	22.08	0.00	8.05

[a] μ_Z, α_{xz}, and α_{yz} are essentially zero for all compounds because of the planar structure. The nonzero values of α_{xz} and α_{yz} obtained for symmetric compounds and the negative values of α_{xz} are due to computational errors.

3.5. Ionization Potentials. The ionization potential energies calculated for the optimized structures of fluoropyrroles are listed in Table 6. Because ionization potential energies are directly proportional to the electrochemical oxidation potentials of the compounds, it can be said that the electrochemical stability of monomer **B** is slightly lower than that of monomer **A** and pyrrole itself so that it undergoes electrochemical oxidation at lower potentials.

3.6. Electric Polarizabilities. Values of exact electrical polarizabilities for the B3LYP/6-31G** optimized structures of all fluoropyrroles have been calculated and are listed in Table 6. Static and dynamic multipole polarizabilities of halogen-containing compounds are important properties needed for the modeling of solvent effects on their reactions in solution. These values are also used to interpret the light scattering and intensities of vibrational Raman spectra of these compounds. The zero values obtained for the α_{xz} and α_{yz} polarizabilities are consequences of the planar structure whereas small values of the α_{xy} polarizabilities indicate that the delocalization strength of the π system of the ring dominates the anisotropic effects of

TABLE 7: B3LYP/6-31G Calculated IR Transition Wavenumbers in cm^{-1} (intensities in km/mol) for Pyrrole and Fluoropyrroles[a]**

molecule	low-frequency range	high-frequency range
pyrrole	461(77), 641(0.98), 734(111), 825(3.5), 875(1.3)	1042(26), 1075(2.3), 1101(8), 1165(2.3), 1180(2.7), 1318(1.9), 1436(4.5), 1470(7), 1517(9), 1594(4), 3247(3.2), 3258(5.7), 3275(7), 3688(55)
A	285(3), 400(72), 415(2.3), 609(4), 660(19), 688(52), 774(55), 888(3), 999(27)	1044(11), 1099(16), 1146(0.8), 1279(5.3), 1290(9), 1434(0.7), 1508(56), 1532(42), 1654(137), 3258(4), 3283(2), 3689(79)
B	315(0.6), 417(86), 619(1.7), 651(11), 655(11), 749(77), 822(7), 892(4), 993(34)	1075(1.9), 1083(18), 1166(6), 1275(14), 1330(61), 1442(21), 1485(13), 1539(6), 1641(90), 3269(0.7), 3693(67)
C	249(2.7), 268(0.9), 307(7.6), 358(78), 476(0.8), 584(7), 630(9), 640(8), 670(39), 748(28), 813(14), 907(21)	1079(6), 1102(48), 1198(32), 1277(3.8), 1348(84), 1444(8.7), 1528(45), 1546(21), 1717(137), 3692(93)
D	224(1), 285(39), 328(2), 401(47), 481(0.9), 581(5.4), 597(1.5), 642(7.8), 668(15), 732(34), 756(75), 987(23.4)	1023(3.5), 1112(15.7), 1174(48.8), 1252(4.4), 1335(29), 1453(56.5), 1520(81.7), 1599(17.2), 1667(218), 3300(1.6), 3308(1.5), 3693(95)
E	220(5),318(73),322(2.4), 492(1.4), 611(9.3), 636(2.2), 696(34), 755(100),	1001(25), 1018(0.5), 1061(22), 1209(38), 1247(2.2), 1465(17), 1486(105), 1624(126), 1679(174), 3280(2.3), 3291(1), 3691(108)
F	257(0.15), 265(0.0), 297(34), 402(69), 492(0.12), 588(0.0), 623(5), 631(2.7), 677(0.0), 747(55.4), 751(28), 897(16)	1071(16), 1136(55), 1210(50), 1274(4), 1369(74), 1449(26), 1492(0.2), 1626(119), 1662(29), 3299(0.8), 3301(0.8), 3702(83)
G	173(13), 200(50), 243(0.14), 296(0.01), 299(1.6), 392(45), 545(1.5), 571(1.2), 586(0.08), 605(20.8), 661(29), 757(25), 770(21)	1062(97), 1097(45), 1256(9.4), 1264(32.8), 1364(74), 1460(49), 1556(70), 1633(70), 1725(111.4), 3309(2.8), 3690(111.2),
H	182(44), 217(15), 256(7), 267(0.9), 321(1.6), 349(20.8), 535(5.6), 585(1.4), 589(1.9), 620(6), 657(10), 746(59), 819(690)	1035(10), 1164(31), 1189(60), 1227(23), 1352(66), 1484(56), 1522(85), 1639(96),1733(172), 3299(3), 3691(124)
I	137(78), 167(0.0), 210(2.6), 37(0.04), 262(0.0), 279(1.1), 304(1.2), 388(26), 527(3), 574(0.0), 579(1.8), 600(1.2), 665(1.2), 765(250), 964(136)	1166(108), 1221(21), 1270(12), 1373(98), 1533(77), 1535(93), 1706(0.8), 1750(183), 3692(142)

[a] Some specific vibrational modes may not be active in IR for certain compounds because of the selection rules arising from symmetrical characteristics.

the substituents for the asymmetric fluoropyrroles. Values of the α_{xy} polarizabilities for symmetric (C_{2v}) fluoropyrroles **E**, **F**, and **I** should essentially be zero.

3.7. Vibrational Spectra. For all systems studied in this work, vibrational frequency calculations were carried out to confirm the local minima on the potential energy surfaces (PESs). The fundamental vibrational frequencies for all fluoropyrroles were calculated using optimized structures at the B3LYP/6-31G** level of theory. In all calculations, we obtained only positive force constants and real frequencies, confirming that the structures correspond to equilibrium points on the PES. The B3LYP/6-31G** calculated IR absorption frequencies and intensities for all fluoropyrroles are presented in Table 7. The frequencies are divided into a low-frequency group (below 1000 cm^{-1}) and a high-frequency group (above 1000 cm^{-1}) to facilitate the comparison. The low-frequency values for all of the compounds except **A** and **B** are smaller than those for pyrrole. Of the two monofluoropyrroles, compound **B** has higher low-frequency values. Also, of the four difluoropyrroles, compound **F** has almost the highest low-frequency values. This means that these two compounds have the largest force constants for their bending modes of vibration, implying that they have less electron−phonon contributions to their electrical resistance. The higher values of low frequencies obtained for **B** and **F** can be regarded as higher protection from thermal decomposition for **B** and **F** compounds compared with that of other fluoropyrroles. Furthermore, this indicates that the relative thermal stabilities of these molecules are higher than those of their corresponding isomers. In terms of the zero-point energy (ZPE), it can be said that the ZPE for molecule **B** is greater than that for molecule **A**. In addition, the value of the ZPE for molecule **F** is greater than that for its isomers—**C**, **D**, and **E**. A more detailed analysis of the comparative thermal stabilities of this series of compounds is reported elsewhere.[28]

Displacements of the C3 and H8 atoms (in Figure 1) for the vibration with the highest intensity in the IR spectrum of fluoropyrroles have been compared in Table 8. It can be seen from this Table that the displacement of the C3 atom for compound **B** is greater than that for its isomer **A**. The same is observed for compound **F** compared with its isomers **C** and **D**. It is important to note that the displacements are given on the basis of the respective standard Cartesian coordinates of the molecules, which may be evidently different from each other.

TABLE 8: Analysis of C3−H8 Displacement (in Å) for the Most Intense Vibrational Mode of Fluoropyrroles in the IR Spectrum[a]

	C3			H8		
molecule	Δx	Δy	Δr	Δx	Δy	Δr
pyrrole	0	0	0.08	0	0	0.50
A	0.13	0.02	0.24	−0.04	0.19	0.19
B	0.17	0.24	0.29	−0.17	0.05	0.56
C	0.10	−0.04	0.11	0.07	0.11	0.13
D	−0.10	−0.22	0.24	0.35	−0.01	0.35
F	0.24	−0.07	0.25	−0.50	−0.07	0.51
G	−0.05	−0.13	0.14	0.15	−0.06	0.16

[a] z displacements for C3 and H8 are zero for all compounds, except for pyrrole, which are 0.08 and −0.5, respectively. The values of Δr have been calculated using the $(\Delta r)^2 = (\Delta x)^2 + (\Delta y)^2 + (\Delta z)^2$ relation.

The displacement of the H8 atom for **B** is smaller than that for **A**, and for **F** it is smaller than that for **C** and **D**. Furthermore, the force constant for the C3−H8 bond in molecules **B** and **F**, because of their higher relative stabilities, must be greater than that for their corresponding isomers. On the basis of the vibrational analysis carried out in this study, it can be predicted that the electropolymerization of fluoropyrroles can be enhanced, or even controlled, by the use of appropriate selective IR radiation.

3.8. NMR Chemical Shifts. The NMR chemical shifts can be used to predict ring currents and estimate the aromaticity in this series of fluoropyrroles. In this study, the ^{1}H and ^{13}C chemical shieldings have been calculated for the DFT-B3LYP/6-31G** optimized geometries of all fluoropyrroles. The isotropic and anisotropic magnetic shieldings for these two nuclei have been calculated using IGAIM, SGO, and CSGT methods. Because of the broad lines of the ^{14}N NMR signal

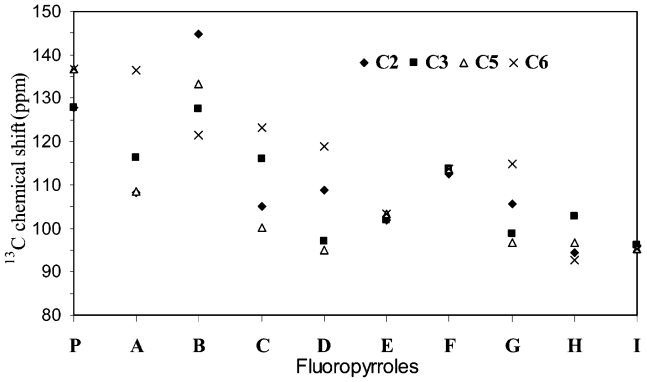

Figure 3. IGAIM calculated values of ^{13}C chemical shifts $\delta_X = \Delta\sigma_X$ referenced to TMS for all carbon atoms in pyrrole **P** and fluoropyrroles **A**−**I** (Figure 1) based on the B3LYP/6-31G** optimized structures.

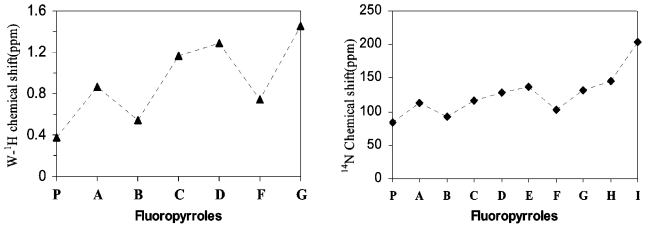

Figure 4. IGAIM calculated values of chemical shifts $\delta_H = \Delta\sigma_H$ of ^{1}H for the hydrogen atom at position W referenced to TMS (left) and of ^{14}N for the nitrogen atom referenced to nitromethane (right) in pyrrole and fluoropyrroles based on the B3LYP/6-31G** optimized structures. Obviously, compounds **E**, **H**, and **I** are absent in the proton chemical shift data because of the lack of the W hydrogen.

and the low natural abundance of ^{15}N, shielding constants for the nitrogen nucleus are not of considerable experimental importance.

An analysis of the calculated shielding constants for the ^{1}H and ^{13}C nuclei shows that the IGAIM and CSGT methods provide similar results for all of the tensorial components of the shielding constants of both nuclei. The isotropic and anisotropic chemical shielding constants are defined as $\sigma_{iso} = (\sigma_{xx} + \sigma_{yy} + \sigma_{zz})/3$ and $\Delta\sigma = \sigma_{zz} - (\sigma_{xx} + \sigma_{yy})/2$, respectively. The ^{1}H and ^{13}C chemical shieldings for TMS have also been calculated as references. On a comparative basis, the relative shielding constant $\Delta\sigma_X$ (i.e., chemical shift δ_X) is defined as

$$\delta_X = \Delta\sigma_X = \sigma_X(\text{reference}) - \sigma_X(\text{fluoropyrrole}) \quad (3)$$

where σ_X(fluoropyrrole) and σ_X(reference) are isotropic chemical shielding constants, σ_{iso}, of nucleus X in the fluoropyrrole and in the reference molecules, respectively. The calculated values of the relative shielding constants, $\Delta\sigma_X$, or chemical shifts, δ_X, for different carbon nuclei in pyrrole **P** and fluoropyrroles **A**−**I** are demonstrated in Figure 3. It can be seen from this Figure that the C2 nucleus has the highest magnetic shielding in compound **B**, the same compound that has the higher capacity for electropolymerization (section 3.3). The C2 carbon atom is the same carbon atom that has the lowest positive charge as well (Table 4). In addition, shielding constants for the C3 nucleus of compounds **B** and **F** are larger than that for the C3 nucleus of other fluoropyrroles.

The left part of Figure 4 shows changes in the values of chemical shifts for the hydrogen nucleus on the W position (W-^{1}H) of the fluoropyrroles (Figure 1). As this Figure clearly shows, the highest values of the ^{13}C NMR chemical shift belong to the W-hydrogen nuclei of compounds **B** and **F**. In addition, with the increase in the number of substituted fluorine atoms on the pyrrole ring, the NMR chemical shifts of all nuclei decrease. The same trend is obtained for the calculated chemical shifts of the ^{14}N nitrogen nucleus referenced to the nitrogen nucleus of nitromethane. These NMR data can be used to probe the electropolymerization or chemical polymerization experimentally based on one or two characteristic nuclei.

4. Conclusions

Fluoropyrroles have been designed as monomers for conductive polymers in the hope of having modified chemical and electrical properties. The primary advantage of the conductive polyfluoropyrroles over their parent polymer, polypyrrole, is their higher pyrolysis temperature, which decreases the risk of fire in the electronic/electrical devices made of these materials. Ab initio and density functional theory DFT-B3LYP/6-31G** calculations have been carried out successfully to study the structural, electronic, electrochemical, and spectroscopic properties of all fluoropyrroles. On the basis of the B3LYP/6-31G** optimized structural parameters, especially the quinoid character, charge distribution, size and direction of the electric dipole moment vector, and vibrational frequencies, it was shown that compounds **B** and **F** are possible candidates to replace pyrrole in the synthesis of corresponding conducting polymers with modified characteristics compared to polypyrrole. Compared to pyrrole, **B** and **F** fluoropyrrole monomers are more soluble in water and have a lower potential energy to form cations. These characteristics increase the efficiency of the electrochemical polymerization processes on these two monomers. Moreover, polymers of these monomers will probably have less zigzag character because of the preferred local charges on the C_α and $C_{\alpha'}$ carbon atoms (C2 and C3 positions in Figure 1).

From the higher values of the vibrational bending modes' frequencies obtained for 3-fluoropyrrole **B** and 3,4-difluoropyrrole **F**, it can be predicted that the electrical resistance parameters of these two compounds have fewer contributions from phonon−electron interactions compared with those of other fluoropyrroles.

Other aspects of the properties of these compounds, especially the thermodynamic and electrical characteristics, have been studied computationally and will be presented in an independent paper.[28] The feasibility of the synthesis of fluoropyrroles and the experimental measurement of their molecular and thermochemical stability are interesting subjects that are open to study.

The molecular modeling methodology successfully used in the present study can be used in any systematic computational search for new compounds with desired characteristics. Furthermore, it has been shown how the prediction of polymer characteristics from the molecular properties of the constituting monomers is possible via quantum mechanical computations.

Acknowledgment. We thank the University of Isfahan and the University of Mazandaran for financial support and research facilities. We gratefully thank Professors A.C. and M.J. for allowing us to use their software and hardware facilities via the Internet.

References and Notes

(1) Vidal, J. C.; Garcia, E.; Castillo, J. R. *Anal. Chim. Acta* **1999**, *385*, 213.

(2) Campbel, T. E.; Hodgson, A. J.; Wallace, G. G. *Electroanalysis* **1999**, *11*, 215.

(3) Kincal, D.; Kamer, A.; Chield, A. D.; Reynold, R. J. *Synth. Met.* **1998**, *92*, 53.

(4) Kemp, N. T.; Flanagan, G. U.; Kaiser, A. B.; Trodahl, H. J.; Chapman, B.; Partridge, A. C.; Buckley, R. G. *Synth. Met.* **1999**, *101*, 434.

(5) Smela, E. *J. Micromech. Microeng.* **1999**, *9*, 1.

(6) Meyer, W. H.; Kiess, H.; Binggeli, B.; Meier, E.; Harbeke, G. *Synth. Met.* **1985**, *10*, 255.

(7) *Handbook of Conducting Polymers*; Skotheim, T. A., Ed.; Marcel Dekker: New York, 1986; Vol. 15.

(8) *Handbook of Conducting Polymers*; Skothiem, T. A., Elsenbaumer, R., Reynolds, J., Eds.; Marcel Dekker: New York, 1998.

(9) Wallace, G. G.; Spinks, G.; Teasdale, P. R. *Conductive Electroactive Polymers: Intelligent Materials Systems*; Technomic: New York, 1997.

(10) Torres-Gomez, G.; Skaarup, S.; West, K.; Gomez-Romero, P. *J. Electrochem. Soc.* **2000**, *147*, 2513−2516.

(11) Chiang, C. K. *Polymer* **1981**, *22*, 1545.

(12) Su, W.; Iron, J. O. *Synth. Met.* **1998**, *95*, 159.

(13) Lu, W. K.; Elsenbaumer, R. A. *Annu. Technol. Conf. Soc. Plast. Eng.* **1998**, *56*, 1276.

(14) Yurtsever, M.; Yurtsever, E. *Synth. Met.* **1998**, *98*, 221.

(15) Yurtsever, E.; Esenturk, O.; Pamuk, H. O.; Yurtsever, M. *Synth. Met.* **1998**, *98*, 229.

(16) Lukes, V.; Breza, M.; Biskupic, S. *Theor. Chim. Acta* **1999**, *101*, 319.

(17) Ansari, R.; Wallace, G. G. *Polymer* **1994**, *35*, 2372.

(18) Singh, R.; Narula, A. K.; Tandon, R. P. *Synth. Met.* **1996**, *79*, 1.

(19) Parr, R. C.; Yang, W. *Density-Functional Theory of Atoms and Molecules*; Oxford University Press: New York, 1989.

(20) Gross, E. K.; Dreiz, R. M. *Density Functional Theory*; Plenum Press: New York, 1995.

(21) *Modern Density Functional Theory: A Tool for Chemists*; Seminarino, J. M., Polizer, P., Eds.; Elsevier: Amsterdam, 1995.

(22) Englisch, H.; Fieseler, H.; Haufe, A. *Phys. Rev. A* **1988**, *37*, 4570.

(23) Von Barth, U. *Phys. Rev. A* **1979**, *20*, 1693.

(24) Frisch, M. J.; Trucks, G. W.; Schlegel, H. B.; Gill, P. M. W.; Johnson, B. G.; Robb, M. A.; Cheeseman, J. R.; Keith, T.; Petersson, G. A.; Montgomery, J. A.; Raghavachari, K.; Al-Laham, M. A.; Zakrzewski, V. G.; Ortiz, J. V.; Foresman, J. B.; Cioslowski, J.; Stefanov, B. B.; Nanayakkara, A.; Challacombe, M.; Peng, C. Y.; Ayala, P. Y.; Chen, W.; Wong, M. W.; Andres, J. L.; Replogle, E. S.; Gomperts, R.; Martin, R. L.; Fox, D. J.; Binkley, J. S.; Defrees, D. J.; Baker, J.; Stewart, J. P.; Head-Gordon, M.; Gonzalez, C.; Pople, J. A. *Gaussian 94W*; Gaussian, Inc.: Pittsburgh, PA, 1995.

(25) Bauschlinger, C. W.; Partridge, H. *J. Chem. Phys.* **1995**, *103*, 1788.

(26) Dresselhaus, M. S.; Dresselhaus, G.; Eklund, P. C. *Science of Fullerenes and Carbon Nanotubes*; Academic Press: London, 1996, and http://webbook.nist.gov/chemistry/.

(27) Colle, R.; Curioni, A. *J. Phys. Chem. A* **2000**, *104*, 8546.

(28) Sabzyan, H.; Omrani, A. *Submitted Paper*.